Spatial Designs and Properties of Spatial Correlation: Effects on Covariance Estimation

Kathryn M. IRVINE, Alix I. GITELMAN, and Jennifer A. HOETING

In a spatial regression context, scientists are often interested in a physical interpretation of components of the parametric covariance function. For example, spatial covariance parameter estimates in ecological settings have been interpreted to describe spatial heterogeneity or "patchiness" in a landscape that cannot be explained by measured covariates. In this article, we investigate the influence of the strength of spatial dependence on maximum likelihood (ML) and restricted maximum likelihood (REML) estimates of covariance parameters in an exponential-with-nugget model, and we also examine these influences under different sampling designs—specifically, lattice designs and more realistic random and cluster designs—at differing intensities of sampling ($n = 144$ and 361). We find that neither ML nor REML estimates perform well when the range parameter and/or the nugget-to-sill ratio is large—ML tends to underestimate the autocorrelation function and REML produces highly variable estimates of the autocorrelation function. The best estimates of both the covariance parameters and the autocorrelation function come under the cluster sampling design and large sample sizes. As a motivating example, we consider a spatial model for stream sulfate concentration.

Key Words: Effective range; Exponential covariance; In-fill asymptotics; Nugget-to-sill ratio.

1. INTRODUCTION

In most situations, the statistical dependence between observations in a sample collected close together on a landscape is modeled by a parametric covariance function when that dependence cannot be soley accounted for by measured covariates. The regression coefficients and covariance parameters of this spatial regression model are subsequently estimated by, for example, maximum likelihood (ML) or restricted maximum likelihood (REML) (Cressie 1993). In some cases, the covariance function is needed only to the extent that it assists in standard error estimation for regression coefficients and/or in making predictions (i.e., kriging). In other cases, however, practical, physical interpretations of covariance function parameters are equally as important as regression coefficient estimates.

Kathryn M. Irvine is Assistant Professor, Department of Mathematical Sciences, Montana State University, Bozeman, Montana 59717-2400 (E-mail: *georgiti@science.oregonstate.edu*). Alix I. Gitelman is Associate Professor, Department of Statistics, Oregon State University, Corvallis, OR 97331. Jennifer A. Hoeting is Associate Professor, Department of Statistics, Colorado State University, Fort Collins, CO 80523.

Journal of Agricultural, Biological, and Environmental Statistics, Volume 12, Number 4, Pages 450–469
DOI: 10.1198/108571107X249799

Indeed, spatial covariance parameter estimates in ecological settings have been interpreted to describe the spatial heterogeneity or "patchiness" in a landscape that cannot be explained by measured covariates (e.g., Rossi et al. 1992; Bellehumeur and Legendre 1998; Dalthorp et al. 2000; Augustine and Frank 2001; Schwarz et al. 2003; Rufino et al. 2004; Kennard and Outcalt 2006).

Consider the isotropic exponential-with-nugget covariance function

$$C(t) = \begin{cases} \sigma^2 \exp(-\phi t) & \text{if} \quad t > 0, \\ \tau^2 + \sigma^2 & \text{otherwise} \end{cases} \tag{1.1}$$

where $t = ||\mathbf{s}_i - \mathbf{s}_j||$ is the distance between two locations $\mathbf{s}_i$ and $\mathbf{s}_j$. In this parameterization (following Banerjee et al. 2004, p. 29), τ^2 is the nugget, $\tau^2+\sigma^2$ is the sill, and $1/\phi$ is the range parameter. The "effective range" is defined as the distance beyond which the correlation between observations, $\rho(t) = C(t)/C(0)$, is less than or equal to 0.05. Effective range is also sometimes defined in terms of where the semi-variogram, $\gamma(t) = C(0) - C(t)$, reaches 95% of the sill: $\gamma(t) = 0.95(\tau^2 + \sigma^2)$. In the isotropic exponential-with-nugget covariance function the effective range, which we will denote ξ, corresponds under both definitions; namely,

$$\xi = -\frac{1}{\phi} \log \left(0.05 \frac{\tau^2 + \sigma^2}{\sigma^2} \right). \tag{1.2}$$

Numerous authors interpret the effective range in the exponential covariance function as a measure to describe the spatial heterogeneity or "patchiness" in a landscape (e.g., Saetre and Baath 2000; Franklin et al. 2002; Schwarz et al. 2003; Rufino et al. 2004; Kennard and Outcalt 2006). Dalthorp et al. (2000) demonstrated with discrete data that the range and nugget parameters influence the patch configuration on a simulated landscape, although Schabenberger and Gotway (2005, p. 140) questioned the use of the range parameter as an estimate of patch size.

Upon estimating the covariance function parameters of the exponential-with-nugget using a real dataset, we obtained somewhat different estimates of the effective range using ML and REML (see Section 2). This quandary led us to investigate the sensitivity of the covariance function parameter estimates and the estimated covariance function itself to different properties of the spatial correlation and to different sampling designs.

In examining the interplay of the three parameters of the exponential-with-nugget model, several authors have considered the "strength of the spatial correlation" in terms of the nugget-to-sill ratio, $\frac{\tau^2}{\sigma^2+\tau^2}$, and/or in terms of the range parameter, $1/\phi$. Lark (2000) noted that when spatial correlation is weak (by which he meant a large nugget-to-sill ratio and a small range parameter), ML is a better choice compared to method of moments when estimating the covariance parameters in the spherical model. Zimmerman and Zimmerman (1991) demonstrated that REML and ML out-perform other estimation methods when the spatial dependence is weak (by which they mean a small range parameter), although their results are based on the exponential-without-nugget covariance function. In the case of the one-dimensional exponential-with-nugget covariance function, it is known that the product $\sigma^2\phi$ can be consistently estimated (under in-fill asymptotics), but that neither parameter

separately can be consistently estimated (again, under in-fill asymptotics) (Chen et al. 2000; Zhang and Zimmerman 2005).

In other related work, Thompson (2001) compared REML and ML estimates simulated under various sampling designs using the two-parameter Matérn covariance model. She showed that including a nugget parameter may improve the properties of the estimators for data simulated under the no-nugget model with several explanatory variables. Cressie (1993, p. 93) noted that REML is typically preferred to ML in the case of a large number of explanatory variables, relative to the sample size.

There has not been a thorough study of the effect, under different sampling schemes, of spatial correlation—measured in terms of nugget-to-sill ratio, range parameter, or some combination of these—on (a) the estimation of covariance function parameters or (b) the corresponding estimate of the autocorrelation function. Our purpose in this article is not only to investigate the influence of the strength of spatial correlation on ML and REML estimates, but also to examine these influences under different sampling designs—specifically, lattice designs and more realistic random and cluster designs—at differing intensities of sampling ($n = 144$ and 361). Zimmerman (2006) suggested that the optimal spatial design for covariance parameter estimation is one with regularly spaced clusters. He also pointed out, however, that the number and configuration of points within a cluster depends on properties of the spatial correlation.

The article is organized as follows. We describe our motivating example in the next section, in the context of a more general discussion of models for spatial data, and we present some results from the initial covariance parameter estimation. We then describe the spatial designs we use for simulations of spatially correlated data and provide details regarding the simulations themselves. In Section 4 we present results of the simulations and interpretations of these results. We return to the example in Section 5, where we offer some practical suggestions for covariance estimation based on the simulation results.

2. SPATIAL MODEL FOR STREAM SULFATE CONCENTRATION

Beginning in the late 1970s, the effects of surface water acidification caused by atmospheric deposition became one of the leading political and scientific issues in the United States. The major sources of anthropogenic surface water acidification are atmospheric deposition, acid mine drainage, and roadcuts that expose sulfide minerals to air and water (Baker et al. 1991; Herlihy et al. 1990, 1991; Kaufmann et al. 1992). To study the spatial heterogeneity of available surface water acidification data, we modeled the sulfate concentration in streams in the mid-Atlantic U.S. using water chemistry data available from the U.S. Environmental Protection Agency's Environmental Monitoring and Assessment Program (EMAP). We focused on stream sulfate concentration because of its observed positive spatial relationship with atmospheric SO_4^{2-} deposition (Kaufmann et al. 1991). Our data are available at *http://www.stat.colostate.edu/~jah/data*.

The Mid-Atlantic region consists of five southwest-to-northeast trending physiographic regions: the Coastal Plain, Piedmont, Blue Ridge Mountains, Valley and Ridge, and Appalachian Plateau (Herlihy et al. 1993). We used a sample of 322 points located throughout

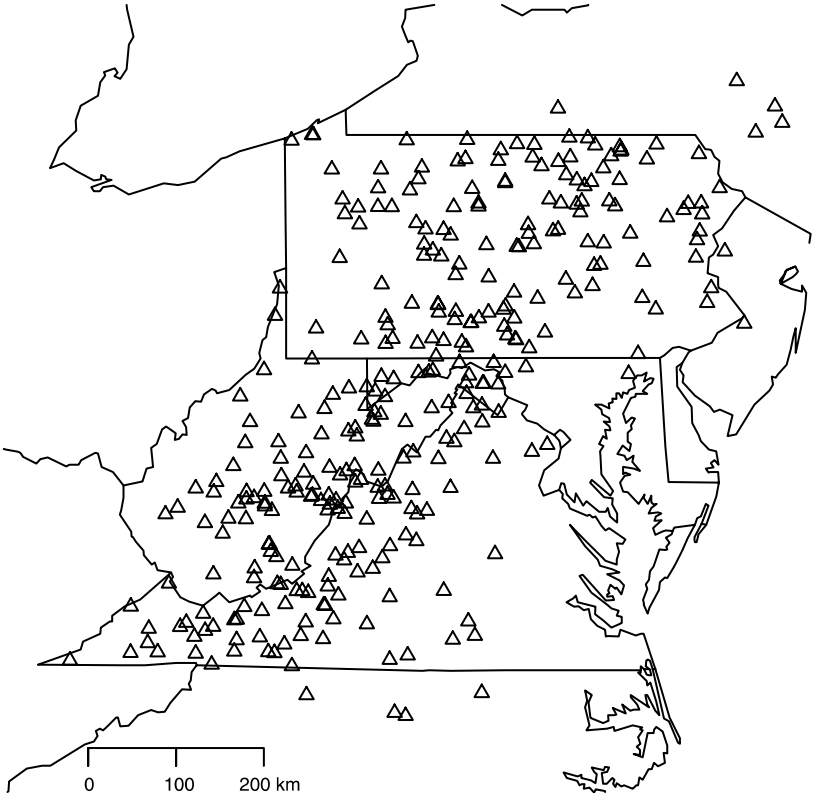

Figure 1. Locations of Mid-Atlantic Highlands Region EMAP Samples.

this region (Figure 1). In addition to water chemistry data, we have potential explanatory variables derived from a Geographic Information System (GIS). The percent of forest, agriculture, urban, and mining within each stream's contributing watershed are calculated from a land-cover map. Another important factor for modeling stream sulfate is the ability of the watershed soils to retain atmospherically deposited sulfur (Herlihy et al. 1993). We calculated, for each watershed, the proportion of that watershed located within the Blue Ridge and Piedmont ecoregions known to have soils with a high capacity for adsorbing sulfate (Herlihy et al. 1993, and Herlihy personal communication)—notice that this proportion is zero for those watersheds not overlapping with Blue Ridge and Piedmont.

Probably the most important component to modeling stream sulfate is the input from atmospheric deposition. This occurs through several mechanisms: wet deposition (rain and snow), dry deposition (direct deposition of particles and gases), and cloud water deposition (direct deposition of cloud and fog droplets; Ollinger et al. 1993). The EMAP data do not contain information about atmospheric deposition at particular stream locations. Instead we used data from the National Atmospheric Deposition Program (NADP) to develop a predictive regression model for wet SO_4^{2-} deposition at stream locations, with the intent of using those predictions as explanatory variables in our model for stream sulfate concentra-

tion. We used precipitation weighted SO_4^{2-} (in equivalents/liter) from NADP monitoring stations within the same geographic region as the EMAP stream locations, only including stations that met the completeness criterion provided by the NADP. Because the stream locations are geographically referenced we were able to use latitude, longitude, and elevation as predictors of wet SO_4^{2-}. This approach is similar to Ollinger et al. (1993); in addition, there was no evidence of spatial correlation in the residuals from our predictive model.

Since we have data from different sources (NADP and EMAP), we used the two-dimensional projection suggested by Banerjee et al. (2004, p. 29) for the predictive wet deposition model and the spatial model of stream sulfate concentration. The Euclidean distance metric applied to this projection's coordinates approximate the geodesic distance between two locations. Thus, instead of using latitude and longitude as predictors of wet deposition, we used the X and Y coordinates from this projection. Also, the intersite distances used in the covariance matrix of the stream sulfate models are based on this projection.

It is worth noting that for covariance modeling we used Euclidean distance instead of distance along the stream network because the greatest source of sulfate in streams is from atmospheric deposition: the covariance between spatial locations is likely to be more influenced by features that would affect atmospheric transport such as, potentially, geography, wind directions, and so on; influences acting across the landscape and not within the stream network. The use of Euclidean distance for this response is also supported by an analysis of a similar dataset where Euclidean distance is preferred as the distance measure in a spatial model as compared to several metrics based on stream distance (Peterson et al. 2006). However, there are situations in which riverine data is analyzed using distance along a stream network (Cressie and Majure 1997; Gardner et al. 2003; Ganio et al. 2005).

2.1 GEOSTATISTICAL MODEL

Let $Z(\mathbf{s}_i)$ denote stream sulfate concentration at location $\mathbf{s}_i$ and assume $\mathbf{Z} = (Z(s_1), \ldots, Z(s_n))'$ are observations on a continuous random field $\mathbf{Z}(\mathbf{s})$ over the finite study area, $\mathbf{D}$, where $\mathbf{s} \in \mathbf{D}$. We consider the geostatistical model for $Z(\mathbf{s}_i)$ given by

$$Z(\mathbf{s}) = \mathbf{X}'(\mathbf{s})\boldsymbol{\beta} + \delta(\mathbf{s}), \tag{2.1}$$

where $\mathbf{X}(\mathbf{s}) = (1, X_1(\mathbf{s}), \ldots, X_p(\mathbf{s}))'$ is a $(p+1)$–length vector of known predictor variables for location $\mathbf{s}$, $\boldsymbol{\beta}$ are the corresponding unknown coefficients, and $\delta(\mathbf{s})$ is the spatial error process at location $\mathbf{s}$. The covariates used to model stream sulfate concentration were the percent of forest, agriculture, urban, and mining within each stream's contributing watershed, the interpolated wet SO_4^{2-} deposition at each location, and the percentage of each watershed located within the Blue Ridge and/or Piedmont ecoregions.

The spatial error $\delta(\mathbf{s})$ is assumed to have a stationary, isotropic, mean-zero Gaussian process with exponential-with-nugget covariance function (1.1). We assessed the validity of the isotropy assumption by investigating empirical semi-variograms for the least squares residuals in different directions: there was no evidence of anisotropy. Because the omnidirectional empirical semi-variogram indicated a vertical displacement from zero we included a nugget term. This accounts for unexplained variability in the response, such as measurement

Table 1. Stream sulfate parameter estimates

	ML	(SE)	REML	(SE)
Intercept	6.07	(2.32)	6.11	(2.36)
Forest	−0.02	(0.02)	−0.02	(0.02)
Agriculture	−0.01	(0.02)	0.01	(0.02)
Urban	0.015	(0.03)	0.015	(0.03)
Mine	0.13	(0.03)	0.13	(0.03)
Wet deposition	0.01	(0.005)	0.01	(0.005)
Ecoregion	−0.01	(0.002)	−0.01	(0.002)
Nugget, τ^2	0.56		0.58	
Partial sill, σ^2	0.47		0.57	
Range, $1/\phi$	89.12		118.79	
Effective range	197.06		272.49	

error or noise. The Gaussian assumption was verified by examining appropriate residual plots.

2.2 PRELIMINARY FINDINGS

After accounting for the association between watershed scale environmental factors and stream sulfate concentration, there remained spatial correlation in the stream sulfate data. Unfortunately, our conclusions about the remaining spatial heterogeneity depended upon the method we used to estimate the covariance parameters—in particular, we were interested in estimating the effective range for this problem. Specifically, the ML estimate of the effective range was 197.06 km, whereas the REML estimate of the effective range was 272.49 km (Table 1). Although these values are not wildly different, they may result in different inferences from an ecological standpoint. For example, one might conclude based on an effective range of 197.06 km that we were unable to account for point sources of sulfate, such as mining and/or roadcuts, using the watershed GIS information. This makes sense because the resolution of the satellite imagery used to create the watershed variables is not fine enough to detect small mines or roads. But if we were to use the REML estimate of effective range of 272.49 km, we might conclude that not only did we not account for the small scale sources of sulfate but we also may have missed important watershed characteristics.

In this analysis the number of covariates ($p = 6$) is small compared to the sample size ($n = 322$), so we would have expected little difference between the REML and ML estimates (Cressie 1993, p. 93). It seems likely that the true value of ϕ in (1.1) for our data is quite small; thus perhaps the difference between the ML and REML estimate of the effective range is somehow due to the strong spatial correlation (i.e., large range parameter). Lark (2000) and Zimmerman and Zimmerman (1991) noted ML estimation performs better when the spatial correlation is weak. Neither of these authors, however, explored the exponential-with-nugget model under REML and ML, which is the focus of our interest.

Also in our example, the estimated nugget-to-sill ratio was 0.54 under ML and 0.50 under REML estimation (Table 1), so we wondered if the relative size of the nugget was a problem for estimation. Mardia and Marshall (1984) found that adding measurement error to the spherical covariance model increased the variability of the ML estimates of the range parameter. Swallow and Monahan (1984) found larger ratios of variance components caused severe estimated bias in the MLEs for the one-way random effects model. Thus, there is some evidence that under other models, the ratio of the two variance components (e.g., nugget and partial sill) may influence the performance of the estimation method.

3. SPATIAL DESIGNS AND SIMULATIONS

We simulated spatially correlated data from three different spatial designs: lattice, random, and clustered (Figure 2). We specifically chose the lattice design since most in-fill and increasing domain asymptotic results for the exponential covariance model are based on sampling points on a lattice (Zhang and Zimmerman 2005). Also, for comparison we used a cluster design, which Zimmerman (2006) and others (Zhu and Stein 2005; Zhu and Zhang 2006) have found to be the optimal design for covariance parameter estimation of the exponential-with-nugget model. Finally, we included the random design because the EMAP sample, which prompted this investigation, is similar to a random spatial design. Thompson (2001) and Hoeting et al. (2006) used a similar range of sampling designs.

For each spatial design we used 144 and 361 sample locations on a 10×10 unit square. Webster and Oliver (2001, pp. 89–90) suggested 144 as an adequate sample size to reliably estimate the parameters for a Gaussian isotropic covariance function. We used 361 to examine in-fill asymptotic properties of the estimates. To assess the influence of properties of spatial correlation on covariance estimation we varied both the nugget-to-sill

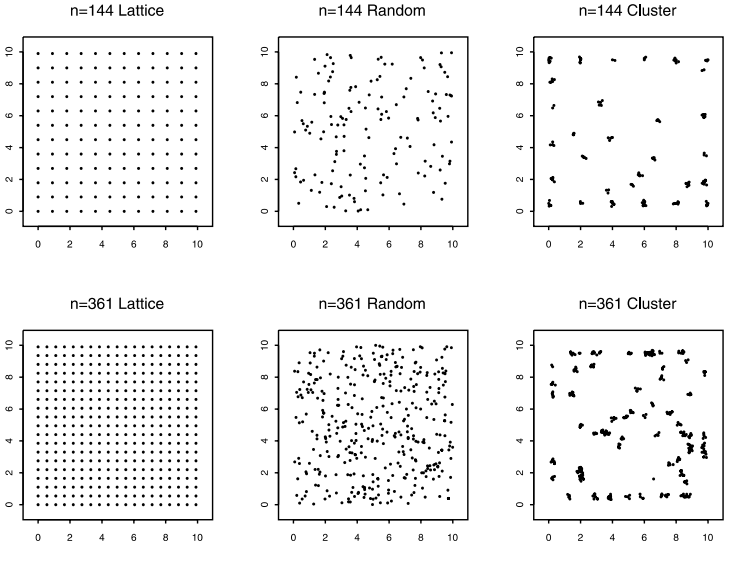

Figure 2. Spatial designs used for simulations.

Table 2. Effective range values used in simulations

Range Parameter	Nugget-to-Sill Ratio $\left(\frac{\tau^2}{\sigma^2+\tau^2}\right)$				
$(1/\phi)$	0.10	0.33	0.50	0.67	0.90
1	2.89	2.59	2.30	1.90	0.69
3	8.67	7.77	6.90	5.70	2.07

ratio and the range parameter. We explore a spectrum of nugget-to-sill ratios (0.10, 0.33, 0.50, 0.67, 0.90), with the sill fixed at 3. Similarly, we selected range parameters $(1/\phi)$ of 1 and 3. The different combinations of nugget-to-sill ratios and range parameters result in a wide variety of effective range values (Table 2), ranging from 0.69 (very weak correlation) to 8.67 (very strong correlation). Note that different parameter combinations can result in similar effective range values. For example, when $1/\phi = 1$ and $\tau^2/(\sigma^2 + \tau^2) = 0.67$ and when $1/\phi = 3$ and $\tau^2/(\sigma^2 + \tau^2) = 0.90$, the effective ranges are quite similar. Details for sample location selection follow for the three spatial designs.

The lattice sample locations were equally spaced over the 10×10 unit square. The minimum distance between sample locations when $n = 144$ was 0.9 and decreased to 0.55 for $n = 361$. The random design sample locations were generated by simulating from a Uniform [0, 10] distribution for each element in $\mathbf{s}_i$, where $\mathbf{s}_i = (x_i, y_i)$ (e.g., longitude and latitude for site $\mathbf{s}_i$). The only difference between the random design with $n = 144$ and 361 is the number of sample locations generated. When $n = 361$ the histogram of pairwise distances for the lattice and random designs were similar.

Cluster designs are found to be the optimal design for spatial covariance estimation by several authors (Pettitt and McBratney 1993; Muller and Zimmerman 1999; Zhu and Stein 2005; Xia et al. 2006; Zimmerman 2006; Zhu and Zhang 2006). Some of these contain "clusters" that are really linear strands of sample points. The values of the range parameter and the nugget-to-partial sill ratio influence the configuration of the clusters in terms of location and number of points within the cluster (Zhu and Stein 2005; Zimmerman 2006; Zhu and Zhang 2006). We have chosen sample locations for our cluster design that mimic the optimal design found by Zimmerman (2006) for covariance parameter estimation. Zimmerman found the optimal design for the exponential-with-nugget model with constant mean and 50% nugget-to-sill ratio had clusters located around the edge of the study region and had a mean cluster size of 2 to 5 points (using a sample size of 50). Our design has 5 to 6 points per cluster, with some clusters located around the periphery and others randomly located throughout the domain. Points that fell outside or on the edge of the domain were resampled until they fell within the specified region. To mimic in-fill asymptotics with $n = 361$ we increased the number of clusters but kept the number of points within the cluster the same. We have only used one cluster design which cannot be optimal for all of the parameter combinations investigated (Zhu and Stein 2005; Zimmerman 2006; Zhu and Zhang 2006).

In the simulations we consider a constant-mean, isotropic Gaussian process with expo-

nential covariance with-nugget function. The model can be expressed as in (2.1) with $\mathbf{X}'(\mathbf{s})\boldsymbol{\beta}$ replaced by μ, for a constant mean structure. For each of the ten combinations (five nugget-to-sill ratios and two range parameters) we simulated 100 realizations under each spatial design and sample size using the RandomFields package in R (*http://www.r-project.org/*). For each realization we obtained the ML and REML estimates of the covariance parameters and μ for each realization using R code from Ver Hoef (2004). We obtained similar estimates when we used the `likfit()` command available in the geoR package for R.

4. RESULTS

We now describe effects of changing sampling design, nugget-to-sill ratio, range parameter, and sample size, using the various simulations described earlier. We first discuss the effects of these changes on estimates of the effective range, ξ, in (1.2) and on estimates of the individual covariance parameters, σ^2, τ^2, and $1/\phi$ from (1.1). We then report the effects of the simulated changes on estimates of the entire autocorrelation function.

4.1 PARAMETER ESTIMATION

For each design/range parameter/sample size/ratio combination, we computed the difference between the estimated effective range and the true effective range. The results shown in Tables 3 (for $1/\phi = 1$) and 4 (for $1/\phi = 3$) are the percentiles of these errors over all simulations. For example, the first line of Table 3 gives results for the 0.10 nugget-to-sill ratio, under the lattice design.

When $1/\phi = 1$, the REML estimator generally has slightly smaller estimation error (50th percentile) than the ML estimator—but surprisingly, much worse estimation error variance, particularly in the 90th percentile (Table 3). ML under-estimates the effective range for all the designs, both sample sizes, range parameters, and most nugget-to-sill ratios—this is consistent with Zimmerman and Zimmerman (1991) who explored the exponential-without-nugget model for a lattice design. When the overall variability is dominated by measurement error (nugget-to-sill ratio = 0.90), the distributions of REML estimators of the effective range are quite heavy-tailed and the corresponding distributions of ML estimators are skewed to the left. The skewness decreases with an increase in sample size, particularly for the cluster design.

The almost universally poor performance of both estimators when $1/\phi = 3$ is somewhat surprising (Table 4)—although both Lark (2000) and Zimmerman and Zimmerman (1991) seem to suggest that the ML estimates should be worse with a stronger spatial correlation. The 90th percentile of the REML estimates of the effective range completely breakdown for all designs, and this problem is not substantially alleviated by an increase in sample size. For both estimation methods the effective range estimates are further from the truth when $1/\phi = 3$ as opposed to 1, or when the nugget-to-sill ratio is 0.90 as opposed to something smaller. The poor performance of the estimators when the nugget-to-sill ratio is large may result from the effective range being negative for nugget-to-sill ratios greater than 0.95—indeed, ratios this large may suggest using a nonspatial (i.e., independent) model.

Simulation results for the nugget, partial sill, and range parameter (τ^2, σ^2, and $1/\phi$,

Table 3. Estimation error for effective range when $1/\phi = 1$. The estimation error is the difference between the estimated effective range and the true effective range. We report the percentiles of these errors over 100 simulations for each design/range parameter/sample size/ratio combination.

			$n = 144$			$n = 361$		
			Error percentile			Error percentile		
$\frac{\tau^2}{\sigma^2+\tau^2}$	Design	Method	10%	50%	90%	10%	50%	90%
0.1	lattice	ML	−1.18	−0.03	1.16	−0.88	−0.20	0.76
		REML	−0.93	0.21	3.24	−0.82	0.00	1.11
	random	ML	−1.11	−0.28	0.89	−0.88	−0.25	0.62
		REML	−0.99	−0.04	1.46	−0.79	−0.08	0.92
	cluster	ML	−1.28	−0.31	1.08	−1.01	−0.27	0.94
		REML	−1.17	−0.02	1.79	−0.92	−0.11	1.40
0.33	lattice	ML	−1.12	−0.19	1.14	−0.94	−0.17	1.09
		REML	−1.03	0.07	3.18	−0.83	0.05	1.69
	random	ML	−1.34	−0.35	0.81	−1.01	−0.27	0.62
		REML	−1.20	−0.02	1.59	−0.92	−0.10	1.15
	cluster	ML	−1.46	−0.69	0.70	−1.14	−0.37	1.45
		REML	−1.40	−0.43	1.28	−1.05	−0.13	2.42
0.5	lattice	ML	−1.11	−0.30	1.64	−1.00	−0.41	0.96
		REML	−0.96	0.21	4.11	−0.87	−0.19	1.64
	random	ML	−1.37	−0.61	1.39	−0.86	−0.30	0.78
		REML	−1.26	−0.21	4.63	−0.77	−0.06	1.32
	cluster	ML	−1.48	−0.37	1.07	−1.18	−0.44	0.77
		REML	−1.36	0.06	2.07	−1.06	−0.24	1.33
0.66	lattice	ML	−32.30	−0.53	0.57	−0.97	−0.30	1.03
		REML	−0.96	−0.11	710.04	−0.92	−0.11	2.04
	random	ML	−1.26	−0.49	1.16	−0.98	−0.32	1.05
		REML	−1.12	−0.04	7.54	−0.92	−0.09	2.14
	cluster	ML	−1.50	−0.64	1.42	−1.12	−0.23	1.02
		REML	−1.38	−0.31	2.98	−1.05	0.04	1.88
0.9	lattice	ML	−371.96	−26.84	0.85	−359.92	−0.20	0.48
		REML	−458.60	0.39	3569.81	−300.49	0.10	502.84
	random	ML	−171.14	−0.39	0.96	−341.89	−0.16	0.59
		REML	−432.89	0.13	1994.30	−295.10	0.06	1390.17
	cluster	ML	−417.23	−0.53	0.72	−7.21	−0.30	0.65
		REML	−514.43	−0.04	4019.94	−1.04	−0.02	30.84

respectively)—not included here—also provide some interesting insight into the interplay between properties of spatial correlation, spatial designs, and estimation. For estimation of the nugget, the cluster design performs best in terms of estimation error percentiles using both ML and REML. However, for all simulations the nugget is fairly well-estimated using both ML and REML. For the estimates of the partial sill and range parameter the REML estimates are more skewed in the 90th percentile when compared to ML estimates, particularly for the larger nugget-to-sill ratios and for $1/\phi = 3$. Also, the ML estimates for the range parameter tend to underestimate the true value, whereas the REML estimates

Table 4. Estimation error for effective range when $1/\phi = 3$. The estimation error is the difference between the estimated effective range and the true effective range. We report the percentiles of these errors over 100 simulations for each design/range parameter/sample size/ratio combination.

			$n = 144$			$n = 361$		
			Error percentile			Error percentile		
$\frac{\tau^2}{\sigma^2+\tau^2}$	Design	Method	10%	50%	90%	10%	50%	90%
0.1	lattice	ML	−5.30	−2.75	4.38	−4.79	−2.18	2.31
		REML	−4.91	−1.51	15.63	−4.40	−0.86	9.89
	random	ML	−5.29	−3.18	2.78	−4.48	−2.01	3.02
		REML	−4.73	−1.88	11.62	−4.03	−0.58	10.89
	cluster	ML	−5.38	−1.94	3.46	−5.07	−2.45	3.98
		REML	−4.86	0.24	13.42	−4.66	−0.74	12.75
0.33	lattice	ML	−5.21	−2.90	3.54	−4.29	−2.27	2.05
		REML	−4.69	−0.90	39.33	−3.82	−0.76	8.77
	random	ML	−5.66	−3.11	2.41	−4.90	−2.37	2.01
		REML	−5.38	−1.28	25.26	−4.40	−0.72	11.34
	cluster	ML	−5.44	−3.37	3.26	−4.96	−2.86	1.67
		REML	−5.02	−1.86	16.40	−4.48	−1.44	11.57
0.5	lattice	ML	−5.02	−2.89	2.18	−4.55	−2.67	2.31
		REML	−4.54	−0.92	62.85	−3.97	−1.21	12.38
	random	ML	−5.38	−3.06	2.24	−4.75	−2.22	1.14
		REML	−5.05	−0.88	43.33	−4.27	−0.46	13.87
	cluster	ML	−5.24	−2.78	2.67	−5.08	−2.75	1.99
		REML	−4.67	−1.21	14.24	−4.80	−1.05	26.73
0.66	lattice	ML	−4.42	−3.30	0.73	−4.40	−2.32	3.86
		REML	−4.13	−0.97	1904.01	−4.17	−0.83	26.75
	random	ML	−4.88	−2.81	1.91	−4.53	−2.58	3.16
		REML	−4.59	0.19	1658.11	−4.26	−1.31	52.54
	cluster	ML	−5.06	−3.02	1.90	−4.18	−2.00	2.85
		REML	−4.57	−1.37	20.48	−3.67	−0.46	23.17
0.9	lattice	ML	−373.34	−1.22	0.79	−37.75	−1.31	0.77
		REML	−459.98	0.19	3545.66	−2.18	−0.10	2464.44
	random	ML	−207.94	−1.47	1.52	−30.42	−1.34	0.84
		REML	−434.27	−0.46	2949.10	−2.15	−0.14	726.00
	cluster	ML	−418.61	−1.88	0.10	−2.53	−1.40	1.63
		REML	−366.30	0.11	6679.31	−1.91	0.35	1255.04

tend to overestimate it. This pattern is more noticeable when $1/\phi = 3$ and the nugget-to-sill ratio is 0.90. Again, for all designs, range parameters, and nugget-to-sill ratios, an increase in sample size improves the estimation error variability for both REML and ML estimates of the partial sill and range parameter.

Perhaps the similarity of the results for the partial sill and range parameter are not surprising given the consistency result regarding the product $\sigma^2\phi$ (Chen et al. 2000; Zhang and Zimmerman 2005). We observed less estimation error skewness for the product $\sigma^2\phi$ using REML compared to ML (results not shown). Interestingly, there is less estimation error variability when $1/\phi = 3$ compared to when $1/\phi = 1$, which is the opposite for both

parameters separately. Also, an increase in sample size improved the estimation error 50th percentile under both procedures.

In terms of correlation, the partial sill and range parameter estimators display a positive association that appears to be primarily driven by outlier estimates (the association is more pronounced when $1/\phi = 3$). The positive association diminishes somewhat when $n = 361$. This positive association actually translates to a negative association between the partial sill and ϕ—perhaps explaining the better estimation of $\sigma^2\phi$ when $1/\phi = 3$, since small estimates of ϕ are associated with large estimates of σ^2, and these may "cancel out" when considering the product. There is a positive association between estimates of $1/\phi$ (range parameter) and partial sill-to-sill ratio, large estimates of $1/\phi$ are associated with partial sill-to-sill ratio estimates close to 1.

4.2 ESTIMATES OF THE AUTOCORRELATION FUNCTION

For each combination of factors (design, nugget-to-sill, range parameter, and sample size), we estimated the spatial autocorrelation function (ACF) using ML and REML. For each of the sampling designs we display the results for the nugget-to-sill ratio of 0.10 using eight panels of plots, each containing a series of boxplots (Figures 3, 4, and 5). Each boxplot summarizes the 100 ACF estimates at a particular distance based on 100 simulations. The solid line in each plot shows the true ACF. We use the following convention in Figures 3, 4, and 5: (a) the top four panels display simulation results for $1/\phi = 1$ and the bottom four panels display results for $1/\phi = 3$; (b) the four left-hand panels correspond to $n = 144$, and the four right-hand panels to $n = 361$; (c) the rows alternate the estimation methods—ML is displayed in the first row, REML in the second row, and so on.

4.2.1 Lattice Design

Figure 3 shows the ACF estimates from ML and REML estimates based on 100 simulations from a lattice design for nugget-to-sill ratio of 0.1. In the top four panels of Figure 3, with $1/\phi = 1$, the estimation of the ACF by ML and REML shows more variability at smaller distances than at larger distances but otherwise performs well. This problem diminishes when the sample size is 361 (compare left and right). However, for $1/\phi = 3$ (bottom four panels), both the ML and REML ACF estimates are flawed. Those based on ML (first column, third row) suffer from underestimation and those based on REML have high variation (first column, fourth row). When the sample size is increased (comparing bottom four panels: left to right), the underestimation of the ACF by ML is not improved, but the variability in the REML estimates of the ACF is reduced; this is true for all nugget-to-sill ratios. For example, when distance between sample locations equals 2, the boxplots for the ACF based on the REML estimates spans the entire range from 0 to 1 (first column, fourth row). While not presented here, the poor performance of both estimation methods with the larger range parameter is seen for all nugget-to-sill ratios and sample sizes.

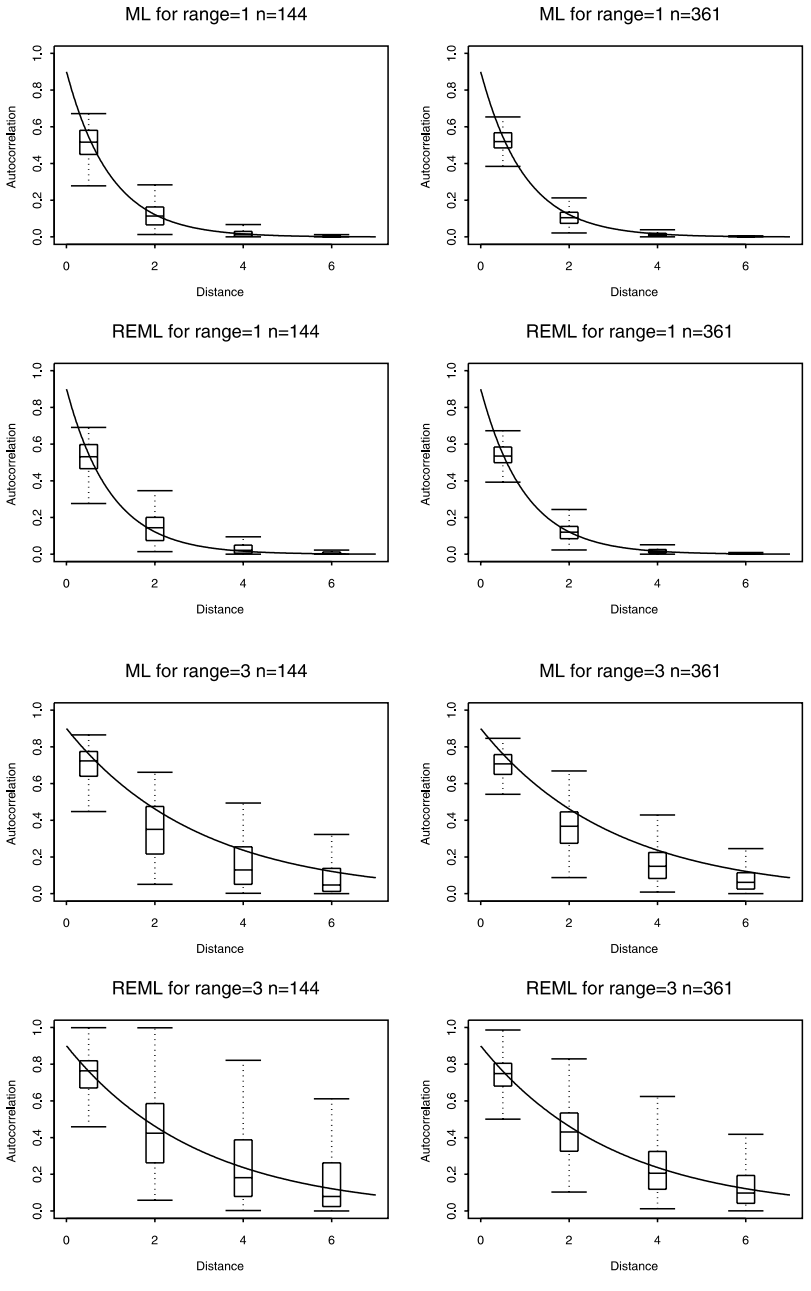

Figure 3. Lattice design: Autocorrelation function estimates from ML and REML based on 100 simulations from a lattice design for nugget-to-sill ratio of 0.10 with sample size and range values as shown. Each boxplot summarizes the 100 autocorrelation function estimates at a particular distance based on the 100 simulations. The solid line in each plot shows the true ACF.

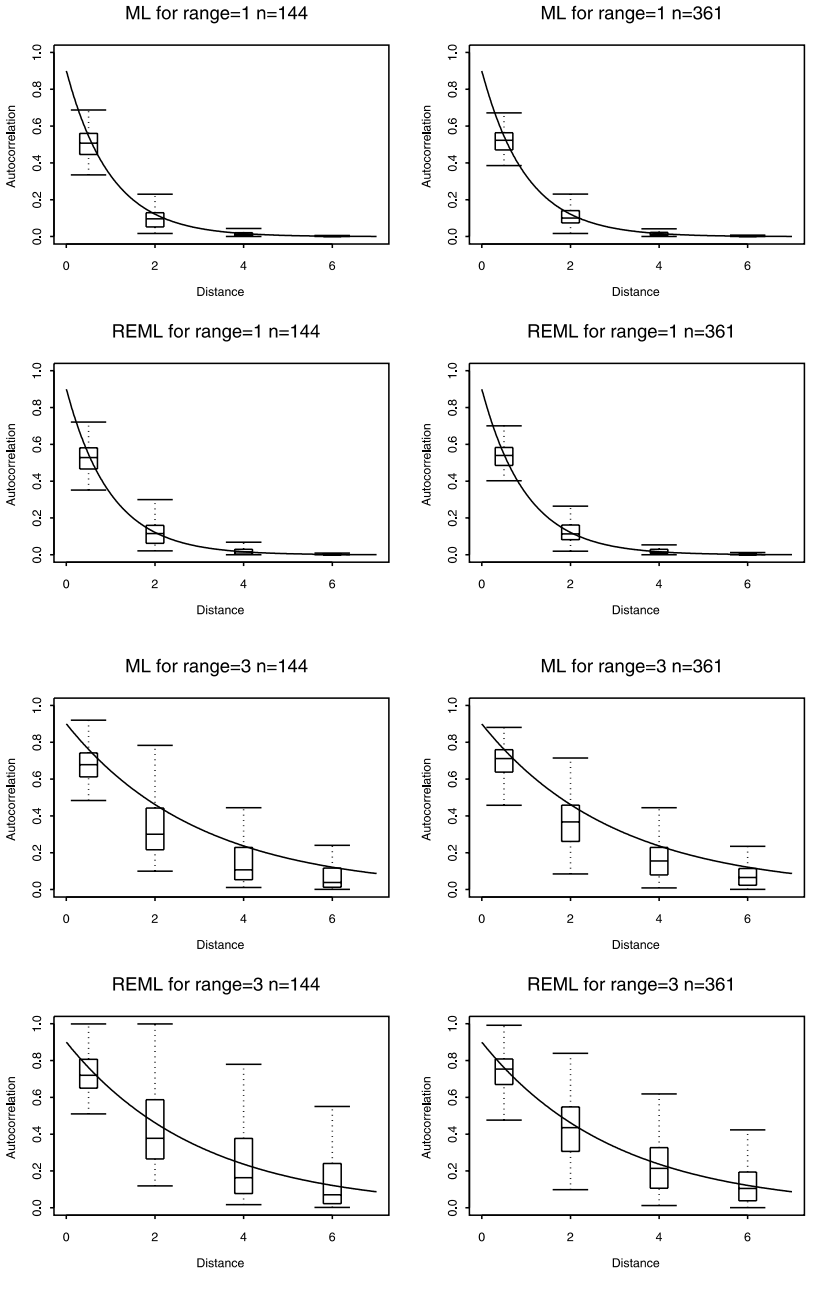

Figure 4. Random design: Autocorrelation function estimates from ML and REML based on 100 simulations from a random design for nugget-to-sill ratio of 0.10 with sample size and range values as shown. Each boxplot summarizes the 100 autocorrelation function estimates at a particular distance based on the 100 simulations. The solid line in each plot shows the true ACF.

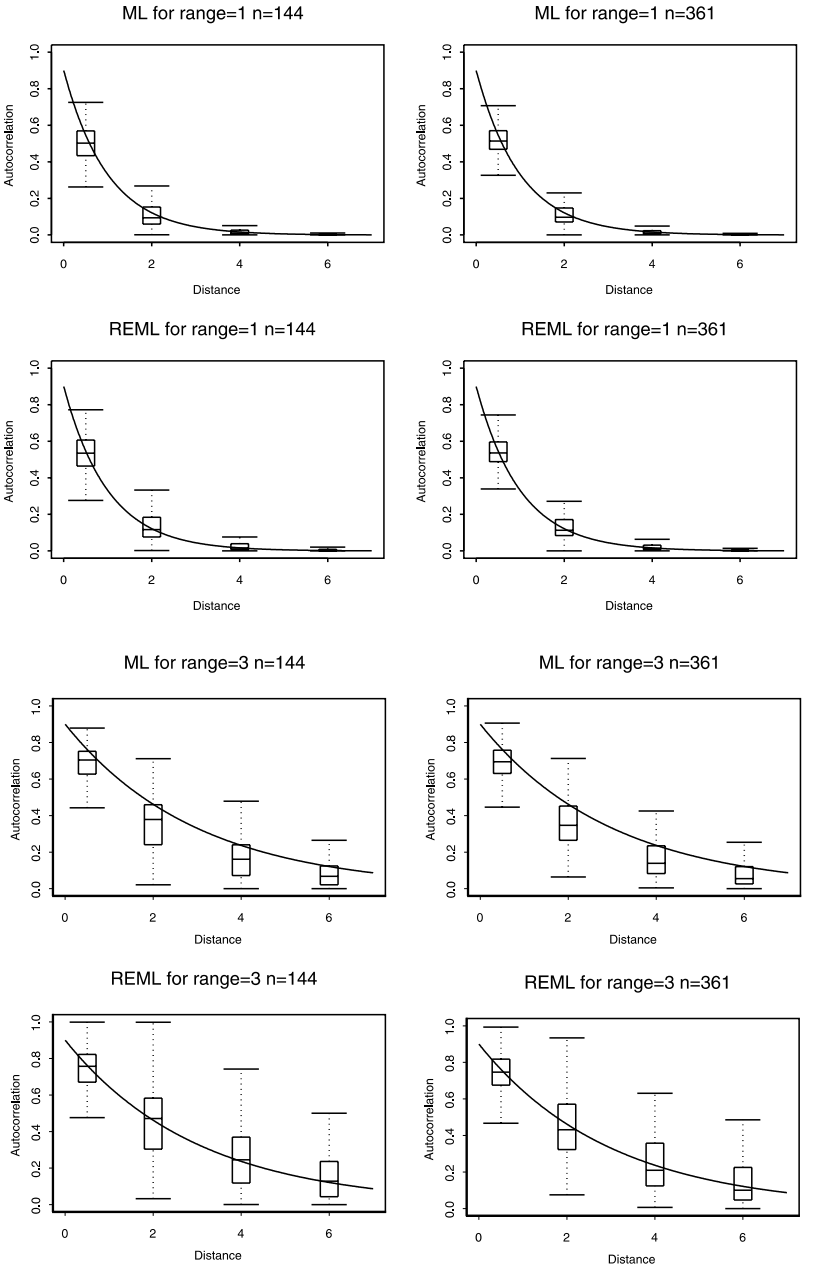

Figure 5. Cluster design: Autocorrelation function estimates from ML and REML based on 100 simulations from a cluster design for nugget-to-sill ratio of 0.10 for sample size and range parameter as labeled. Each boxplot summarizes the 100 autocorrelation function estimates at a particular distance based on the 100 simulations. The solid line in each plot shows the true autocorrelation function.

4.2.2 Random Design

Figure 4 shows the ACF estimates from ML and REML based on 100 simulations from a random design for nugget-to-sill ratio of 0.1. For $1/\phi = 1$ (top four panels), the ACF estimates based on ML and REML are quite good for both sample sizes. These patterns are the same for all nugget-to-sill ratios investigated. As with the lattice design, when $1/\phi = 3$ ML underestimates the ACF and REML produces highly variable estimates of the ACF (bottom four panels); similar results are found for the other nugget-to-sill ratios (not displayed). There is an improvement in terms of variability when the sample size is increased (comparing bottom four panels: left to right).

4.2.3 Cluster Design

Once again, we use the same simulation settings as before to report results for the cluster design in Figure 5. For ML and REML estimates with $1/\phi = 1$ the variability in the estimated ACF decrease as the distance between points increases, following the same pattern as in the lattice and random designs. When $1/\phi = 3$, both estimators have larger variances, with very high variability for the estimates of the ACF using REML. For all nugget-to-sill ratios, when $n = 144$ and $1/\phi = 3$, ML underestimates the true ACF. Increasing the sample size to 361 does not alleviate the problems with large variability in the REML estimates or underestimation by ML; this is also true for the other ratios investigated.

5. DISCUSSION

For all designs, sample sizes, and nugget-to-sill ratios ML and REML produce reasonable estimates of the ACF in terms of estimation error and variability when $1/\phi = 1$. Referring back to Table 2, $1/\phi = 1$ corresponds mostly to lower effective range values. When $1/\phi = 3$ (mostly larger effective range values), however, ML tends to produce low estimates and REML tends to produce highly variable estimates of the ACF for both sample sizes. This corroborates Minasny and McBratney (2005), who compared REML and weighted nonlinear least squares estimates of Matérn covariance parameters. We believe this can have substantial effects in real studies, and we now return to the stream sulfate example to match up our simulation results with estimates we obtained in that study.

The stream sulfate example of Section 2 most closely matches the simulation exercise under the random spatial design with $n = 361$ (recall that $n = 322$ in the stream sulfate example). We compare our motivating example with the simulation results based on the range parameter and the nugget-to-sill ratio estimates because the pattern in the simulations were most easily explained by the magnitude of the range parameter and the nugget-to-sill ratio.

The estimated nugget-to-sill ratio under both REML and ML was approximately 0.50 (refer to Table 1). Comparing the estimated range parameter values from the stream sulfate data to those used for the simulations is a little more difficult because the measurements are on different scales. To facilitate this comparison, we rescaled the distances in the stream sulfate data to a 10×10 unit grid, and then reestimated all parameters using both ML and

REML. Using the rescaled distances, we estimate $1/\phi$ in the stream sulfate example under ML to be 1.14 or $\phi = 0.88$, and under REML to be 1.52 or $\phi = 0.66$.

Notice that this REML estimate of $1/\phi$ using the rescaled distances (i.e., 1.52), falls between our simulation values of 1 and 3, so perhaps it is not surprising that we see a slight discrepancy between the ML and REML estimates of the effective range in the stream sulfate data (recall that these were 197.06 and 272.49, for ML and REML, respectively). This discrepancy is not as dramatic as some of the simulation results because of the large sample size in the stream sulfate data, and because the effective range is perhaps not as large as in some of the simulated cases. Really it seems that the stream sulfate example falls on the boundary of where ML and REML are fairly similar and fairly well-behaved in terms of estimating the covariance parameters.

Recalling that ML tends to under-estimate the effective range when the range parameter $(1/\phi)$ is large, and that REML tends to have high variability in the same case (Table 4), the practitioner can make a more informed decision on which estimation procedure to use, based on the risks inherent in each. In general terms, for reasonable nugget-to-sill ratios (less than 0.90) and larger values of the range parameter $(1/\phi)$, ML estimates would likely be preferred because of the unacceptable estimation error variability for REML.

The results presented here support and enhance previous findings about optimal spatial designs (Pettitt and McBratney 1993; Muller and Zimmerman 1999; Zhu and Stein 2005; Xia et al. 2006; Zimmerman 2006; Zhu and Zhang 2006). The cluster design performed the best in terms of estimating the ACF and the covariance parameters individually. This observation is based on plotting the median and interquartile range of the ACF for all three designs simultaneously. The cluster design tended to have the same or a narrower interquartile range compared to the other designs. The estimates could possibly be improved by selecting designs for the specific parameter combinations investigated, although in practice this is not often possible. We chose a design that should be optimal for nugget-to-sill ratios of 0.50, and in general we found the cluster design was as good if not better than the lattice and random designs at these settings. Additional support for the cluster design was given by Hoeting et al. (2006) and Thompson (2001) who found that a cluster design performs well when the goal is model selection of explanatory variables in a geospatial regression model.

All designs when $1/\phi = 1$ (which roughly corresponds to a relatively small effective range) and the sample size is large ($n = 361$) are similar in terms of estimating the autocorrelation function using either ML or REML estimation. The sample sizes that we chose (144 and 361) are really quite large considering that many practitioners deem anything larger than a sample size of 30 to be "large." Webster and Oliver (2001, pp. 89–90) suggested a sample size of 144 as the *minimum* required to reliably estimate parameters for a Gaussian isotropic covariance function. Our results suggest that even 144 may be too few data points if both the range parameter and the nugget-to-sill ratio are large.

Estimates of uncertainty for spatial covariance parameter estimates can be based on in-fill or increasing domain asymptotic results—our simulations mimic in-fill asymptotics. Cressie and Lahiri (1996) provided sufficient conditions for REML estimates of spatial covariance parameters to be consistent and asymptotically Normal under the increasing domain framework; however, there are not similar results available under the in-fill asymp-

totic framework. Zhang and Zimmerman (2005) found the Normal approximation would be inappropriate for the distribution of the MLE of the range parameter. Currently, it is not clear what practitioners should use as a variance estimate of the range parameter and/or the effective range.

In this article we focus on the estimation and interpretation of spatial covariance parameters; however, another area of interest for practitioners could be prediction of stream sulfate at unobserved locations. Stein (1988) found that for the exponential-without-nugget covariance function the product $\sigma^2\phi$ must be estimated well for efficient prediction. This is supported by the consistency results for the exponential-without-nugget model (Zhang 2004; Zhang and Zimmerman 2005), which show the product of the parameters is consistent but the individual parameters are not, under in-fill asymptotics. Madsen (2000) found when the true range parameter is large, REML estimation using an alternative parameterization based on Stein's (1988) work performs better compared to the parameterization used in our model. However, Zhang and Zimmerman (2005) used the alternative parameterization and found the MLE for the inverse range was still highly skewed. It is not clear if an alternative parameterization based on the consistency results would alleviate the poor performance we found for REML estimation.

While we have focused on ML and REML estimation, a comment regarding Bayesian estimation is warranted (Banerjee et al. 2004, pp. 129–170). Our results may illuminate some of the difficulties encountered in fitting equivalent Bayesian models with covariance function (1.1), for example. In fitting these models via Markov chain Monte Carlo methods, it can be difficult to obtain convergence of the covariance parameters, particularly the range parameter. In particular, the large variation we see in many of the REML estimates for the larger range parameter may manifest as convergence problems in the Bayesian framework.

ACKNOWLEDGMENTS

Research supported in part by U.S. Environmental Protection Agency STAR Research Assistance Agreements CR-829095 awarded to Colorado State University and CR-829096-01 awarded to Oregon State University. EPA does not endorse any products or commercial services mentioned here. The views expressed here are solely those of the authors. The authors thank Alan Herlihy, Lisa Madsen, Andrew Merton, Scott Urquhart, and Jay Ver Hoef for useful discussions. The Associate Editor and two anonymous reviewers provided insightful comments that led to an improved article.

[Received January 2006. Revised April 2007.]

REFERENCES

Augustine, D. J., and Frank, Douglas A. (2001), "Effects of Migratory Grazers on Spatial Heterogeneity of Soil Nitrogen Properties in a Grassland Ecosystem," *Ecology*, 82, 3149–3162.

Baker, L. A., Herlihy, A. T., Kaufmann, P. R., and Eilers, J. M. (1991), "Acidic Lakes and Streams in the United States: The Role of Acidic Deposition," *Science*, 252, 1151–1154.

Banerjee, S., Carlin, B. P., and Gelfand., A. E. (2004), *Hierarchical Modeling and Analysis for Spatial Data*, Boca Raton, FL: Chapman and Hall/CRC Press.

Bellehumeur, C., and Legendre, P. (1998), "Multiscale Sources of Variatio in Ecological Variables: Modeling Spatial Dispersion, Elaborating Sampling Designs," *Landscape Ecology*, 13, 15–25.

Chen, H.-S., Simpson, D. G., and Ying, Z. (2000), "Infill Asymptotics for a Stochastic Process Model With Measurement Error," *Statistica Sinica*, 10, 141–156.

Cressie, N., and Majure, J. J. (1997), "Spatio-Temporal Statistical Modeling of Livestock Waste in Streams," *Journal of Agricultural, Biological, and Environmental Statistics*, 2, 24–47.

Cressie, N. A. C. (1993), *Statistics for Spatial Data*, New York: Wiley.

Cressie, N. A. C., and Lahiri, S. N. (1996), "Asymptotics for REML Estimation of Spatial Covariance Parameters," *Journal of Statistical Planning and Inference*, 50, 327–341.

Dalthorp, D., Nyrop, J., and Villani, M. (2000), "Foundations of Spatial Ecology: The Reification of Patches Through Quantitative Description of Patterns and Pattern Repetition," *Entomologia Experimentalis et Applicata*, 96, 119–127.

Franklin, R. B., Blum, L. K., McComb, A. C., and Mills, A. L. (2002), "A Geostatistical Analysis of Small-Scale Spatial Variability in Bacterial Abundance and Community Structure in Salt Marsh Creek Bank Sediments," *FEMS Microbiology Ecology*, 42, 71–80.

Ganio, L. M., Torgensen, C. E., and Gresswell, R. E. (2005), "A Geostatistical Approach for Describing Spatial Pattern in Stream Networks," *Frontiers in Ecology and Environment*, 3, 138–144.

Gardner, B., Sullivan, P. J., and Lembo, Jr., A. J. (2003), "Predicting Stream Temperatures: Geostatistical Model Comparison using Alternative Distance Metrics," *Canadian Journal of Fisheries and Aquatic Science*, 60, 344–351.

Herlihy, A. T., Kaufmann, P. R., Church, M. R., Wigington, Jr., P. J., Webb, J. R., and Sale, M. J. (1993), "The Effects of Acidic Deposition on Streams in the Appalachain Mountain and Piedmont Region of the mid-Atlantic United States," *Water Resources Research*, 29, 2687–2703.

Herlihy, A. T., Kaufmann, P. R., and Mitch, M. E. (1990), "Regional Estimates of Acid Mine Drainage Impact on Streams in the mid-Atlantic and Southeastern United States," *Water, Air, and Soil Pollution*, 50, 91–107.

——— (1991), "Stream Chemistry in the Eastern United States 2. Current Sources of Acidity in Acidic and Low Acid-Neutralizing Capacity Streams," *Water Resources Research*, 27, 629–642.

Hoeting, J. A., Davis, R. A., Merton, A. A., and Thompson, S. E. (2006), "Model Selection for Geostatistical Models," *Ecological Applications*, 16, 87–98.

Kaufmann, P. R., Herlihy, A. T., and Baker, L. A. (1992), "Sources of Acidity in Lakes and Streams of the United States," *Environmental Pollution*, 77, 115–122.

Kaufmann, P. R., Herlihy, A. T., Mitch, M. E., Messer, J. J., and Overton, W. S. (1991), "Stream Chemistry in the Eastern United States 1. Synoptic Survey Design, Acid-Base Status, and Regional Patterns," *Water Resources Research*, 27, 611–627.

Kennard, D. K., and Outcalt, K. (2006), "Modeling Spatial Patterns of Fuels and Fire Behavior in a Longleaf Pine Forest in the Southeastern USA," *Fire Ecology*, 2, 31–52.

Lark, R. M. (2000), "Estimating Variograms of Soil Properties by the Method-of-Moments and Maximum Likelihood," *European Journal of Soil Science*, 51, 717–728.

Madsen, L. J. (2000), "Comparing Two Parameterizations of the Exponential Variogram in REML Parameter Estimation and Spatial Prediction," unpublished master's thesis, Cornell University, Ithaca, New York.

Mardia, K., and Marshall, R. (1984), "Maximum Likelihood Estimation of Models for Residual Covariance in Spatial Regression," *Biometrika*, 71, 135–146.

Minasny, B., and McBratney, A. B. (2005), "The Matérn Function as a General Model for Soil Variograms," *Geoderma*, 128, 192–207.

Muller, W. G., and Zimmerman, D. L. (1999), "Optimal Designs for Variogram Estimation," *Environmetrics*, 10, 23–37.

Ollinger, S. V., Aber, J. D., Lovett, G. M., Millham, S. E., Lathrop, R. G., and Ellis, J. M. (1993), "A Spatial Model of Atmospheric Deposition for the Northeastern U.S." *Ecological Applications*, 3, 459–472.

Peterson, E. E., Merton, A. A., Theobald, D. M., and Urquhart, N. (2006), "Patterns of Spatial Autocorrelation in Stream Water Chemistry," *Environmental Monitoring and Assessment*, 121, 569–594.

Pettitt, A. N., and McBratney, A. B. (1993), "Sampling Designs for Estimating Spatial Variance Components," *Applied Statistics*, 42, 185–209.

Rossi, R. E., Mulla, D. J., Journel, A. G., and Franz, E. H. (1992), "Geostatistical Tools for Modeling and Interpreting Ecological Spatial Dependence," *Ecological Monographs*, 62, 277–314.

Rufino, M. M., Maynou, F., Abello, P., and Yule, A. B. (2004), "Small-Scale Non-linear Geostatistical Analysis of *Liocarcinus depurator* (crustacea:brachyura) Abundance and Size Structure in a Western Mediterranean Population," *Marine Ecology Progress Series*, 276, 223–235.

Saetre, P., and Baath, E. (2000), "Spatial Variation and Patterns of Soil Microbial Community Structure in a Mixed Spruce-Birch Stand," *Soil Biology and Biochemistry*, 32, 909–917.

Schabenberger, O., and Gotway, C. A. (2005), *Statistical Methods for Spatial Data Analysis*, Boca Raton, FL: Chapman and Hall/CRC Press.

Schwarz, P. A., Fahey, T. J., and McCulloch, C. E. (2003), "Factors Controlling Spatial Variation of Tree Species Abundance in a Forested Landscape," *Ecology*, 84, 1862–1878.

Stein, M. L. (1988), "Asymptotically Efficient Prediction of a Random Field with a Misspecified Covariance Function," *The Annals of Statistics*, 16, 55–63.

Swallow, W. H., and Monahan, J. F. (1984), "Monte Carlo Comparison of ANOVA, MIVQUE, REML, and ML Estimators of Variance Components," *Technometrics*, 26, 47–57.

Thompson, S. E. (2001), "Bayesian Model Averaging and Spatial Prediction," unpublished PhD thesis, Colorado State University, Fort Collins, CO.

Ver Hoef, J. (2004), Graybill Conference, June 16–18. In *Short Course on Spatial Statistics*, Fort Collins, CO.

Webster, R., and Oliver, M. A. (2001), *Geostatistics for Environmental Scientists*, West Sussex, England: Wiley.

Xia, G., Miranda, M. L., and Gelfand, A. E. (2006), "Approximately Optimal Spatial Design Approaches for Environmental Health Data," *Environmentrics*, 17, 363–385.

Zhang, H. (2004), "Inconsistent Estimation and Asymptotically Equal Interpolations in Model-Based Geostatistics," *Journal of the American Statistical Association*, 99, 250–261.

Zhang, H., and Zimmerman, D. L. (2005), "Towards Reconciling two Asymptotic Frameworks in Spatial Statistics," *Biometrika*, 92, 921–936.

Zhu, Z., and Stein, M. L. (2005), "Spatial Sampling Design for Parameter Estimation of the Covariance Function," *Journal of Statistical Planning and Inference*, 134, 583–603.

Zhu, Z., and Zhang, H. (2006), "Spatial Sampling Design Under the Infill Asymptotic Framework," *Environmetrics*, 17, 323–337.

Zimmerman, D. L. (2006), "Optimal Network Design for Spatial Prediction, Covariance Parameter Estimation and Empirical Prediction," *Environmetrics*, 17, 635–652.

Zimmerman, D. L., and Zimmerman, M. B. (1991), "A Comparison of Spatial Semivariogram Estimators and Corresponding Ordinary Kriging Predictors," *Technometrics*, 33, 77–91.